Infrared spectroelectrochemical investigations on the doping of soluble poly(isothianaphthene methine) (PIM)

H. Neugebauer, C. Kvarnström,[a] C. Brabec, and N. S. Sariciftci
Physical Chemistry, Johannes Kepler University of Linz, Altenbergerstraße 69, A-4040 Linz, Austria

R. Kiebooms
Instituut voor Materiaal Onderzoek, Materiaalfysica, Limburgs Universitair Centrum, Wetenschapspark 01, B-3590 Diepenbeek, Belgium

F. Wudl
Department of Chemistry and Biochemistry, University of California, Los Angeles, California 90095

S. Luzzati
Instituto di Chimica delle Macromolecole, CNR, Via Bassini 15, I-20133 Milano, Italy

(Received 8 January 1999; accepted 2 April 1999)

Attenuated total reflection Fourier transform infrared (ATR-FTIR) investigations on the doping processes in substituted poly(isothianaphtene methine) (PIM), a new low band-gap conjugated polymer, are reported. The doping was studied *in situ* during chemical *p*-doping (oxidation) by iodine and during electrochemical *p*-doping (oxidation) and *n*-doping (reduction). During both signs of doping, infrared active vibrational (IRAV) bands due to strong coupling of the electrons to lattice vibrations are observed. The results are compared to FT-Raman spectra. Electrochemical *p*-doping shows two different doping regimes depending on the electrochemical potential. The narrow linewidth and low absorption intensities of the IRAV bands indicate a strong localization of the doping induced charge carriers, which is ascribed to a tilted geometry of the conjugated backbone due to steric repulsion effects. © *1999 American Institute of Physics.* [S0021-9606(99)51924-7]

I. INTRODUCTION

The genuine interest in conducting and semiconducting conjugated polymers stems from the fact that they offer the opportunity to combine the electrical properties of metals with the low cost, large scale processability of plastics in a single material. Many applications are envisioned. Low tech applications such as intrinsically antistatic plastics, plastics for shielding the electromagnetic interference (EMI), and secondary battery electrodes are already in use or industrially demonstrated. Recently large scale interest arose for the electroluminescence of conjugated polymers which will enter the market of light emitting diodes very soon.[1–3] Plastic solar cells are another photonic application which might be of great importance in the near future as cheap photovoltaic elements.[4–8] In all these photonic device applications there is an additional advantage of conjugated polymers as active materials: the possibility of band-gap engineering. Due to chemical modification of the conjugated polymer backbone, as well as chemical functionalization of the backbone with different sidechains, there is a practically infinite parameter space which can be utilized to alter the electronic properties of these organic semiconductors. An important parameter of design is thereby the value of the energy gap which separates the completely filled valence band (π-band) from the completely empty conduction band (π^*-band). It has been shown that through chemical engineering on the basis of functional side groups, interring torsion angles, and aromaticity, the value of the energy gap can be varied by several electron volts.[9,10] This is an important feature for application purposes, for example to adjust the color of light emitting diodes. Another important direction of this band-gap engineering in conjugated polymeric semiconductors is to achieve low band-gap materials. This direction is threefold important:

(i) First, the number of intrinsic charge carriers which are thermally excited from the valence band to the conduction band scales exponentially with the band gap. The lower the band gap, the higher the undoped room temperature conductivity.
(ii) Second, the infrared regime for light emission is very attractive for telecommunication bands.
(iii) Low band-gap materials are needed for maximum photon harvesting in the solar cell applications as well as for competition with silicon ($E_{\mathrm{gap}}=1.15$ eV) in photodetector applications.

A number of calculations indicate that in systems which possess a degenerate ground state (like trans-polyacetylene), the band-gap value increases as a function of bond length alternation (i.e., the difference between single and double bond lengths).[11] Brédas *et al.* investigated this problem for nondegenerate ground state conjugated polymers (like polythiophene, polypyrrole, polyparaphenylene, etc.) via valence effective Hamiltonian (VEH) calculations by varying their geometries from aromatic to quinoid-like.[12,13] The evolution is such that the band-gap decreases linearly when quinoid

[a]Permanent address: Åbo Akademi University, Laboratory of Analytical Chemistry, Åbo, Finland.

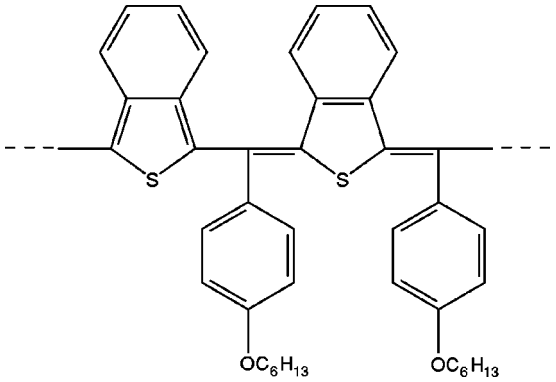

FIG. 1. Schematic structure of poly(isothianaphthene methine) (PIM).

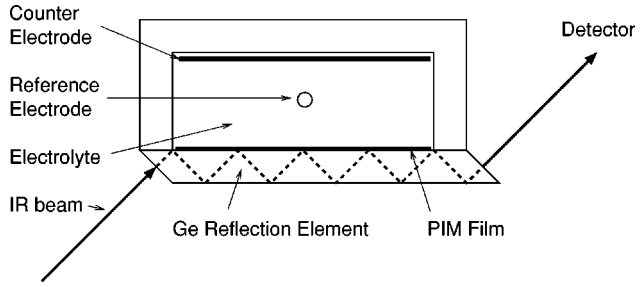

FIG. 2. Spectroelectrochemical cell for *in situ* ATR-FTIR spectroscopy.

character is increasing. After a sharp minimum the band gap increases again upon further increase of the quinoid character. These calculations confirmed the results obtained by Wudl *et al.* in the preparation of polyisothianaphthene (PITN).[14] PITN can be thought of as a thiophene unit with a benzene ring fused at 3,4 positions, and indeed shows a band gap of around 1.0 eV compared to unsubstituted polythiophene with a band gap around 2.5 eV. The disadvantage of PITN lies in the very high reactivity of the monomer as well as instability of the polymer towards ambient conditions. Up until now, PITN remained as a material of academic interest, therefore new low band-gap materials with ambient stability as well as processability are still of great importance.[15]

Another direction to obtain low band-gap materials is the realization of alternating aromatic and quinoid thiophene units along the chain. Poly(heteroarylene methines) were presented by Jenekhe *et al.*[16–18] The band gap of a model compound, 5,5′-bithiophenemethenyl, was calculated to be 1.21 eV.[19] In a combination of both approaches (fused thiophene units in an alternating aromatic and quinoid structure), the band gap of poly(biisothianaphthene methine) was calculated as 0.7 eV.[20]

Key properties for application of conjugated polymers are processibility and stability of the substances. Solubility and fusibility can be achieved by side chain substitution. Recently, a soluble derivative of poly(isothianaphthene methine), poly[(benzo⟨*c*⟩thiophene-1,3-diyl)(p-(hexyloxy)benylidene)(benzo ⟨*c*⟩thiophenequinodimethane-1,3-diyl)]) (PIM) was synthesized.[21] The substance can be dissolved in organic solvents like tetrachloroethane and shows good stability under ambient conditions. The schematic structure of the undoped form of PIM is shown in Fig. 1. As one of the very few examples within the conjugated conducting polymer family, PIM is both *p*- and *n*-dopable, which makes the material an attractive candidate for applications where both types of doping are needed (e.g., all polymer secondary batteries).[22]

In this work we show that PIM is a stable, low bandgap conducting polymer that can reversibly be doped of both *p*- and *n*-type electrochemically in organic electrolyte. The *in situ* attenuated total reflection (ATR) Fourier transform infrared (FTIR) spectroscopy[23–25] has been used to study the spectroelectrochemical behavior and the doping induced IRAV absorption bands arising upon electrochemical *p*- and *n*-doping of PIM films. The spectra are compared with IRAV spectra obtained by iodine doping and with FT-Raman spectra. Electrochemical doping shows clearly two different *p*-doping mechanisms and one mechanism at *n*-doping. The results are explained by a strong localization of charge carriers due to steric effects.

II. EXPERIMENT

The synthesis of PIM has been described in the literature.[21] Thin films of PIM were prepared by drop casting from tetrachloroethene solution on the surface of the electrode and dried in vacuum. For the *in situ* spectroelectrochemical investigations, the electrode consisted of a germanium reflection element ($10\times10\times1$ mm) with an electrochemically active area of 0.63 cm^2. The electrolyte was 0.1 M tetrabutylammoniumperchlorate ($TBAClO_4$) in acetonitrile freshly distilled over CaH_2 and purged with argon to exclude oxygen during the electrochemical reactions. For counter and reference electrode, a platinum sheet and a Ag/AgCl electrode were used, respectively. All potential values in this paper refer to the Ag/AgCl reference electrode. The electrochemical equipment consisted of a potentiostat (Jaissle IMP 88 PC), a sweep generator (Prodis 1/14I) and an XY recorder (Philips PM8132). All experiments were done at room temperature. The spectroelectrochemical experiments were performed with a potential sweep rate of 5 mV/s. For comparison, cyclic voltammetric experiments were also done using a platinum electrode with a drop casted PIM film as working electrode. Higher sweep rates up to 100 mV/s were applied in these experiments.

For ATR-FTIR spectroscopy, a Bruker IFS66S spectrometer with an MCT detector was used. The spectra were measured with a spectral resolution of 4 cm^{-1}. The setup for ATR-FTIR spectroelectrochemistry is shown in Fig. 2. Spectral changes were recorded consecutively during slow potential sweeps. To obtain specific spectral changes during individual electrochemical reaction processes, a spectrum just before the considered reaction is chosen as the reference spectrum. The subsequent spectra are related to that spectrum, showing only the spectral differences to the reference state. The difference absorption spectra are calculated as $\Delta(-\log(T_{\mathrm{ATR}}))$ (T_{ATR}=transmission in ATR geometry). Each spectrum covers a range of about 85 mV in the cyclic voltammogram. For iodine doping, thin films of PIM were prepared by drop casting from tetrachloroethane solution on

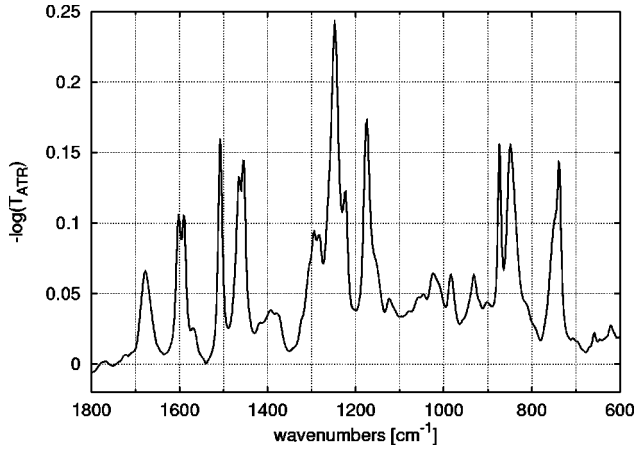

FIG. 3. Neutral form of PIM obtained *in situ* at −300 mV (reference: cell filled with electrolyte).

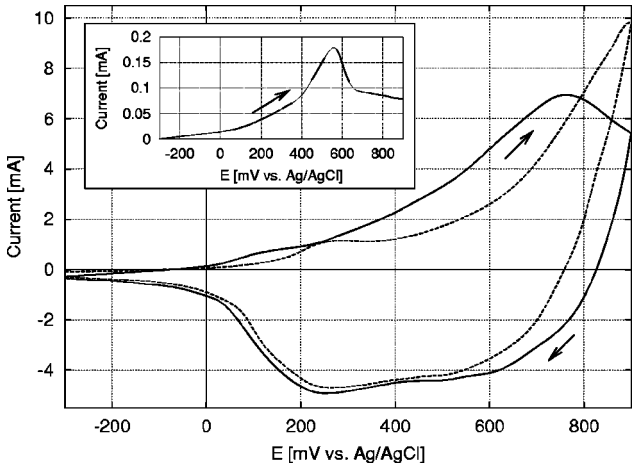

FIG. 4. Cyclic voltammogram of the *p*-doping process. Pt electrode, 100 mV/s. Dashed line: first cycle; solid line: second cycle. Inset: current/voltage curve during the spectroelectrochemical experiment; Ge electrode, 5 mV/s.

the surface of a ZnSe reflection element and dried in vacuum. The sample was mounted in an ATR cell similar to the spectroelectrochemical cell shown in Fig. 2 (without electrodes and electrolyte). The doping was performed by placing iodine into the cell. Before and after the process ATR-FTIR spectra were recorded. To obtain UV-VIS spectra, thin films of PIM were dropcasted on the surface of a quartz substrate and measured with a Hewlett Packard 8453 spectrometer. FT-Raman spectra were obtained using a Bruker FRA106+IFS66 spectrometer with 1064 nm excitation wavelength.

Structure calculations were done by nonlinear conjugate gradient minimization of an input structure using the software package TINKER[26] with parameter set MM3.[27]

TABLE I. IR absorption bands of PIM, neutral form. Intensities: vs: very strong, s: strong, m: medium, w: weak, vw: very weak.

Frequency [cm^{-1}]	Intensity	Comment
3062	w	[a]
3030	vw	[a]
2956	m	shoulder[a]
2933	m	[a]
2871	w	doublet[a]
2858	w	doublet[a]
1678	m	
1603	s	doublet
1589	s	doublet
1566	vw	shoulder
1508	s	
1466	s	doublet
1454	s	doublet
1392	vw	
1296	m	doublet
1282	m	doublet
1248	vs	
1223	w	shoulder
1176	s	
1124	vw	
1024	w	
984	w	
931	w	
874	s	
850	s	
737	s	
658	vw	
621	vw	

[a]Not shown in Fig. 3.

III. RESULTS AND DISCUSSION

A. Neutral PIM

Compared to other substituted polythiophene derivatives, PIM in the neutral state gets oxidized at rather low potentials.[21] Thus, the measurement of a clean infrared absorption spectrum under ambient conditions is hindered by spontaneous oxidation with atmospheric oxygen. To exclude these effects, the spectrum of the neutral form of PIM was measured *in situ* in the spectroelectrochemical cell in contact with the electrolyte solution under applied potential of −300 mV (Fig. 3). The spectrum in Fig. 3 has as reference the identical cell filled with electrolyte, but with no polymer film. In Table I, frequencies and intensities of the

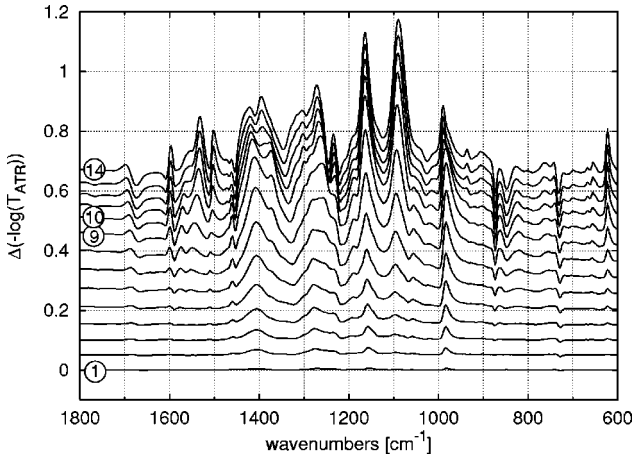

FIG. 5. Difference spectra during *p*-doping. Reference spectrum at −300 mV (neutral form), Ge electrode, 5 mV/s. The spectra are separated. Sequence: bottom to top.

TABLE II. IRAV bands during low *p*-doping. Intensities: vs: very strong, s: strong, m: medium, w: weak.

Frequency [cm^{-1}]	Intensity	Comment
1415	s	
1371	w	shoulder
1278	m	shoulder at high potential
1259	m	shoulder at low potential
1165	vs	
1095	s	ClO_4^-
1055	w	shoulder
985	s	

infrared absorption bands of the neutral form of PIM (Fig. 3) are listed.

B. *p*-doping

Similar to many other conjugated polymers, the first cycle in cyclic voltammetric experiments with PIM shows a different behavior compared to the subsequent cycles due to differences in conformational reorganization of the polymer chain during the redox processes, which are history dependent.[28–30] From the second cycle on, the cyclic voltammograms are stable. In the present paper, the spectroelectrochemical data are from the second cycle.

The cyclic voltammogram of the *p*-doping (oxidation) and dedoping (rereduction) processes is shown in Fig. 4. In the second cycle, the maximum of the *p*-doping current occurs at +750 mV, the dedoping current maximum is found at +250 mV. Figure 5 shows difference spectra during the electrochemical *p*-doping process of PIM on a Ge reflection element as electrode with a sweep rate of 5 mV/s (second cycle). Under this slow scan speed the doping current maximum occurs around +570 mV (inset in Fig. 4). The reference spectrum was taken at −300 mV (neutral form of PIM).

Doping induced IRAV bands show distinctly different dynamics at the ''low doping'' regime (spectra 1 to 9, −300 to +500 mV) compared to the ''high doping'' regime

TABLE III. IRAV bands during high *p*-doping. Intensities: vs: very strong, s: strong, m: medium, w: weak.

Frequency [cm^{-1}]	Intensity	Comment
1697	w	
1597	m	
1562	w	
1531	s	
1502	s	
1437	m	
1396	m	
1331	m	
1306	w	shoulder
1273	m	
1165	s	
1088	vs	ClO_4^-
993	m	
935	w	
908	w	
654	w	
623	m	

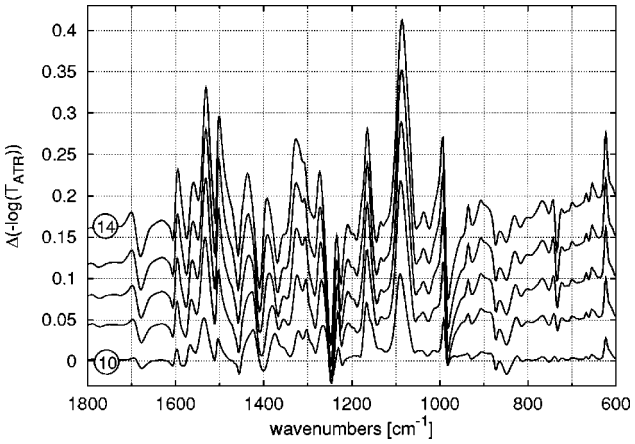

FIG. 6. Difference spectra during high *p*-doping. Reference spectrum at +500 mV (spectrum 9 in Fig. 5). The spectra are separated. Sequence: bottom to top.

(spectra 10 to 14, +600 to +900 mV) as listed in Tables II and III. After spectrum 9 (+500 mV, high *p*-doping regime) the spectral behavior changes significantly. To obtain only the spectral changes during high *p*-doping, Fig. 6 shows the difference spectra 10 to 14 of Fig. 5, but now relative to the spectrum 9 as reference. The bands are listed in Table III.

For comparison, *p*-doping was also performed chemically using iodine as oxidation agent and studied spectroscopically. After measuring the spectrum of the neutral form of PIM on the surface of a ZnSe reflection element, the film was exposed to iodine vapor. The ATR-FTIR spectra of PIM both in the neutral form and doped with iodine are shown in Fig. 7. The bands of iodine doped PIM are listed in Table IV. The spectrum of the neutral form shows an increasing background absorption $>2000\ cm^{-1}$ (not shown in Fig. 7) and small spectral features (marked with arrows in Fig. 7) indicating, that the material is already slightly oxidized due to contact with atmospheric oxygen.

The vibrational spectra of conjugated conducting polymers exhibit strong IRAV bands upon doping, which are correlated to a strong electron–phonon coupling peculiar to

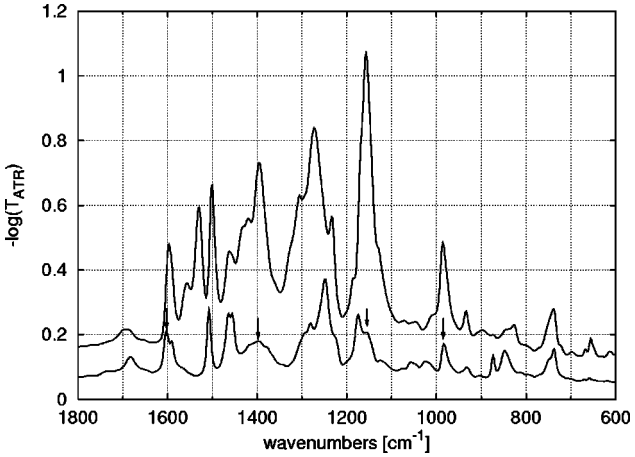

FIG. 7. ATR-FTIR spectra of PIM. Reference spectrum: ZnSe reflection element without polymer. Lower spectrum: neutral form; upper spectrum: iodine doped form. The spectra are separated.

TABLE IV. IRAV bands of iodine doped PIM. Intensities: vs: very strong, s: strong, m: medium, w: weak, vw: very weak.

Frequency [cm^{-1}]	Intensity	Comment
3060	vw	[a]
2954	w	shoulder[a]
2924	m	[a]
2887	vw	shoulder[a]
2852	w	[a]
1699	w	doublet
1684	w	doublet
1599	s	
1558	w	shoulder
1529	s	
1502	s	
1466	m	shoulder
1435	vw	shoulder
1421	vw	shoulder
1396	s	
1308	w	shoulder
1273	s	
1232	w	shoulder
1175	vs	
1070	vw	
1043	vw	
1012	vw	shoulder
985	m	
933	w	
825	w	
737	m	
656	w	

[a]Not shown in Fig. 7.

quasione-dimensional solids.[31] A first attempt to explain these observations has been presented by Horowitz *et al.* for transpolyacetylene.[32,33] The basic concept of the Horovitz theory is to consider the charge density wave which exists in the dimerized form of transpolyacetylene with the fact that π-electrons are coupled to the motion of the polymer backbone. The ''pinning parameter'' is a measure of localization. Zerbi *et al.* showed the correlation of the bands with the infrared activation of totally symmetric modes which contain a contribution by the ''effective conjugation coordinate'' which basically describes the changes of geometry from the ground state to the excited electronic state of the polymer (ECC theory). The smaller the value of the ''effective conjugation force constant'' the larger the ''effective conjugation'' of the polymer backbone.[31] Very recently Ehrenfreund and Vardeny established a link between the doping induced electronic states within the semiconducting $\pi-\pi^*$ energy gap and the IRAV bands of the doping induced infrared spectrum[34] based on a linear response theory by Soos *et al.*[35] Furthermore, there are theoretical descriptions unifying these models.[36] In all the descriptions, there is a strong link between the effective conjugation of the macromolecule, effective delocalization of the doping induced (or photoinduced) quasiparticle excitations such as polarons, solitons, etc., and the signatures of the IRAV bands in the doping induced infrared spectrum. In the framework of the model presented by Zerbi *et al.*,[31,37,38] the IRAV bands correspond to totally symmetric Raman active vibrational A_g modes, which couple to the π-electron system (electron–phonon coupling) along the effective conjugation coordinate (ECC). The vibrations

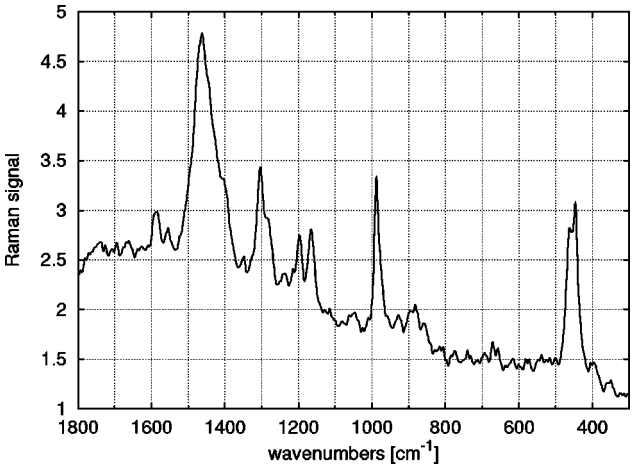

FIG. 8. FT-Raman spectrum of PIM, neutral form. Excitation wavelength 1064 nm.

become infrared active due to symmetry breaking and are strongly enhanced, because the charge distribution in the formed polaronic or bipolaronic state causes high dipole moment changes during vibration. In general, in the frequency range between 1600 and 800 cm^{-1} four A_g modes exist in polythiophene, which, in unsubstituted polythiophenes, give rise to a pattern of three strong bands in the photoinduced absorption spectrum[39] and in the doping induced absorption spectrum[40] as well as to three main Raman bands.[41] For alkyl substituted thiophenes, an additional Raman band around 1000 cm^{-1} occurs.[42]

Raman spectra are highly important for the understanding of vibrational properties and the behavior of IRAV bands in conjugated systems with electron–phonon coupling. The FT-Raman spectrum of the neutral form of PIM, which consists of alternating aromatic and quinoid isothianaphthene units, is shown in Fig. 8. The main bands are listed in Table V. The number of Raman bands is much smaller than the number of vibrational features detected in the IR absorption spectrum of neutral PIM (see Fig. 3). This observation indicates a selective enhancement of the totally symmetric A_g modes strongly coupled to the π-electron structure, characterized by few intense Raman bands. A comparison with literature on Raman spectra of model compounds (isothianaphthenes selectively substituted to force either the aromatic or the quinoid structure)[43] suggests that the FT-Raman pattern mainly corresponds to the aromatic units in

TABLE V. FT-Raman bands of neutral PIM. Intensities: vs: very strong, s: strong, m: medium, w: weak, vw: very weak.

Frequency [cm^{-1}]	Intensity	
1587	w	
1555	vw	
1462	vs	
1304	s	
1198	m	
1165	m	
987	s	
462	m	doublet
446	s	doublet

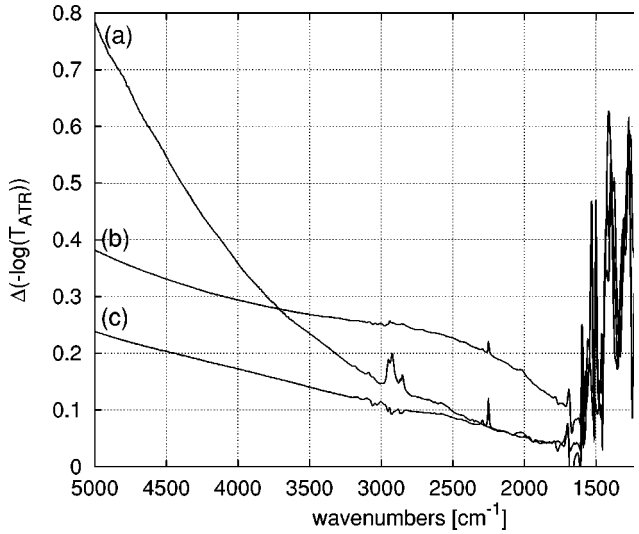

FIG. 9. Comparison of the electronic absorption. (a) Iodine doped, (b) low doping regime, (c) high doping regime. The spectra are scaled to similar intensities in the IRAV band region.

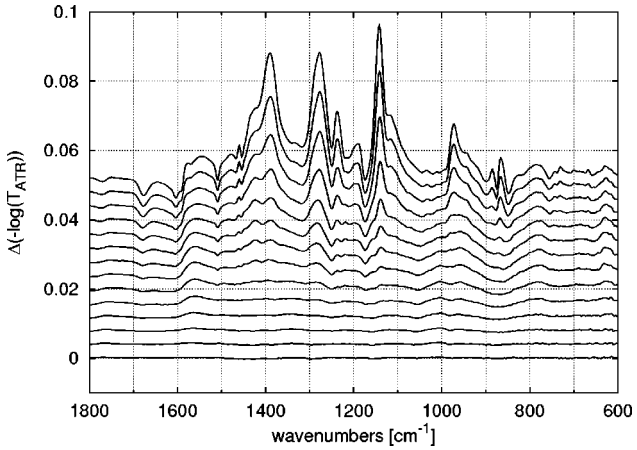

FIG. 11. Difference spectra during *n*-doping. Reference spectrum at −300 mV (neutral form). Ge electrode, 5 mV/s. The spectra are separated. Sequence: bottom to top.

the PIM chains. The bands at 1555 and at 1587 cm^{-1} are associated to C=C stretching at either side of the quinoid isothianaphthene units and to vibration of the aromatic ring in the side chain. The low intensities indicate a weak electron–phonon coupling for these modes.

For spectroelectrochemistry in the low *p*-doping regime, the IRAV spectra are dominated by the evolution of four strong IRAV bands around 1400, 1260–1280, 1165 and 985 cm^{-1}. An additional strong band around 1095 cm^{-1} comes from perchlorate counterions, which are incorporated into the polymer film and balance the positive charges on the chain formed during *p*-doping. Although the force field calculated for polythiophene[31] may not be directly applicable to substituted polythiophenes, the pattern of three main bands (around 1400, 1280–1260, and 1160 cm^{-1}) is also observed in the low *p*-doping regime. The band at 985 cm^{-1} is attributed to the substitution of the thiophene rings. Besides some frequency shifts of the two higher energetic bands, the spectral pattern of the IRAV bands in the low *p*-doping regime corresponds to the FT-Raman spectrum, indicating that mostly aromatic units are involved in the low *p*-doping process.

In contrast, in the high *p*-doping regime the IRAV bands in the region between 1500 and 1600 cm^{-1} can be attributed to C=C vibrations at either sides of the quinoid units.[43] The results show that mainly quinoid rings are involved in the high *p*-doping regime. The IRAV spectrum of PIM doped with iodine looks very similar to the spectroelectrochemical results obtained in the high *p*-doping regime, indicating the redox potential of iodine to be high enough to convert PIM into the highly doped state. The main difference in the spectra of chemical doping to electrochemical doping is the missing absorption band at 1095 cm^{-1} of perchlorate counterions.

The IRAV bands show low intensities compared to IRAV bands of other thiophene containing conjugated polymers. In Fig. 7, the bands of the *p*-doped form are only about 2–3 times higher than the bands of the neutral form. Usually, the factor is about 20–30 found in common thiophene containing conjugated systems. In addition, the band widths are remarkably narrow. The band width at half maximum is around 20–30 cm^{-1} compared to >50 cm^{-1} with other conjugated polymers. The low intensities and the narrow band shapes indicate that the delocalization of the positive charges on the chain is rather low.[44]

In Fig. 9, the electronic absorptions in the low *p*-doped, high *p*-doped, and iodine doped state are compared. A UV-VIS spectrum of iodine doped PIM[21] shows a maximum around 1000 nm (10 000 cm^{-1}) with a long absorption tail at the low energy side, as observed in our spectrum [Fig. 9(a)]. A similar behavior, but with decreased intensity, is found for the electrochemically highly doped state [Fig. 9(c)]. The electronic absorption of the low *p*-doped material [Fig. 9(b)] has an additional broad absorption around 2500 cm^{-1}, again indicating a different mechanism in the low doping regime.

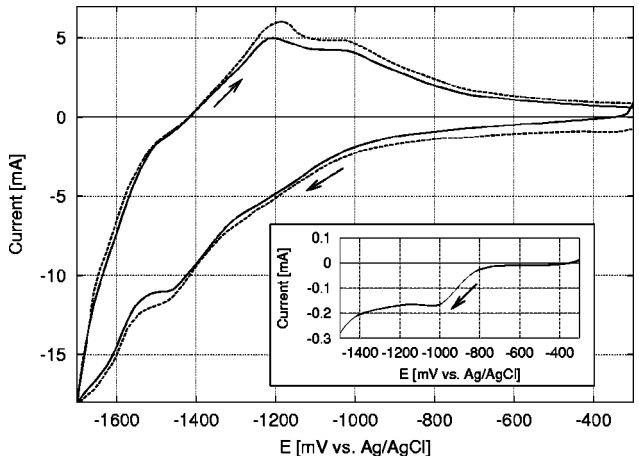

FIG. 10. Cyclic voltammogram of the *n*-doping process. Pt electrode, 100 mV/s. Dashed line: first cycle; solid line: second cycle. Inset: current/voltage curve during the spectroelectrochemical experiment. Ge electrode, 5 mV/s.

TABLE VI. IRAV bands during *n*-doping. Intensities: vs: very strong, s: strong, m: medium, w: weak.

Frequency [cm^{-1}]	Intensity	Comment
1437	w	shoulder
1388	s	
1277	s	
1238	m	
1190	w	
1142	vs	
1115	w	shoulder
974	m	

FIG. 13. Energy minimized structure of a PIM segment. The solid line indicates the conjugation path.

C. *n*-doping

The cyclic voltammogram of the *n*-doping (reduction) and dedoping (reoxidation) processes of PIM is shown in Fig. 10, and the corresponding difference ATR-FTIR spectra in Fig. 11. The IRAV bands arising during electrochemical *n*-doping are listed in Table VI. In contrast to the behavior at *p*-doping, the IRAV bands during electrochemical *n*-doping (reduction) show continuous behavior with much smaller intensities indicating an overall much lower doping level. The spectra obtained during *n*- and low *p*-doping (i.e., the spectral signatures of the charge carriers of both signs) are quite similar. Following the arguments presented in the discussion of *p*-doping above, the pattern of the four main IRAV bands are attributed mainly to the aromatic units in the PIM chain.

D. Estimation of the electronic gap

By comparing the potential values of the electrochemical *p*-doping and *n*-doping processes (electrochemical gap), the calculation of the energy difference between the valence band and the conduction band (electronic gap) in the band structure of the polymer should be possible. In a simple rigid band picture, no charge exchange between the electrode and the polymer will happen, until the applied voltages reaches either the valence band (in that case *p*-doping will appear) or the conduction band (causing *n*-doping). For precise measurements, the sweep rate of the potential should be infinitely low (Electrochemical Potential Spectroscopy),[45] and no side reactions are allowed. From cyclic voltammetric experiments with nonzero sweep rate only estimations can be drawn. Although the determination of the electronic gap from our experiments is difficult due to possible side reactions of the electrolyte solution, the gap is well below 1.5 eV, coinciding with the optical data obtained from the UV-VIS spectrum of a neutral PIM film shown in Fig. 12, where the maximum of the absorption band is found at 2 eV with an onset around 1.5 eV.

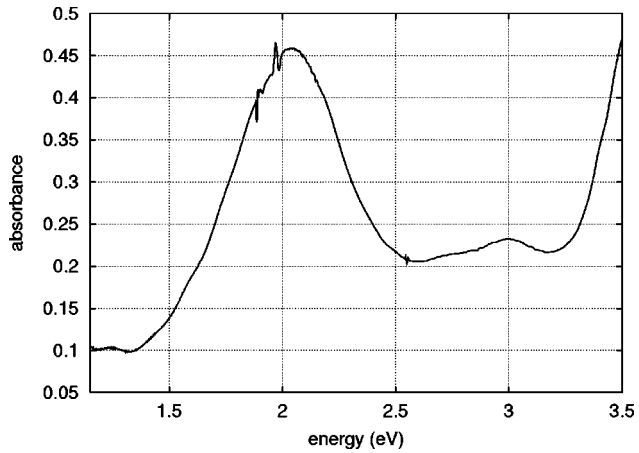

FIG. 12. UV-VIS spectrum of PIM, neutral form. The sharp features are due to spectrometer response.

E. Structure calculations

The results presented in this paper indicate a strong localization of the charges in the doped states of PIM correlated with the low intensities and narrow linewidths of the IRAV bands. Steric repulsion of consecutive units causes strong noncoplanarity, which in turn decreases the effective conjugation and induces charge carrier localization. Structure calculations by nonlinear conjugate gradient minimization[26] are shown in Fig. 13. As can be seen, coplanarity of the conjugated system can hardly be achieved due to the geometric repulsion of the fused heteroaromatic rings and of the large side chains.

IV. CONCLUSION

PIM is a low band-gap material which can be *p*-doped (oxidized) in two different doping processes as well as *n*-doped (reduced) in one process. The electrochemical energy gap is found to be less than 1.5 eV. However, the steric repulsion of the consequent polymer chain units results in a nonplanar configuration, thus a low conjugation and a strong localization of the charge carriers, as clearly seen by the low intensities of the IRAV bands which are unusually narrow. Therefore as such, PIM is a candidate for optical applications for low bandgap materials but with an expected low charge carrier mobility.

ACKNOWLEDGMENTS

The work was supported by the ''Fonds zur Förderung der wissenschaftlichen Forschung'' (FWF) of Austria, Project No. P 12680-CHE. Ch. Etzlstorfer and G. Matt are gratefully acknowledged for their help with geometrical calculations. R. K. is a postdoctoral researcher of the National Science Foundation - Flanders. C. K. was supported by the Research Institute of the Foundation of Åbo Akademi University.

[1] J. H. Burroughes, D. D. C. Bradley, A. R. Brown, R. N. Marks, K. Machay, R. H. Friend, P. L. Burn, and A. B. Holmes, Nature (London) **347**, 539 (1990).
[2] D. Braun and A. J. Heeger, Appl. Phys. Lett. **58**, 945 (1991).
[3] Uniax Corp. (Santa Barbara, USA), Cambridge Display Techn. (Cambridge, UK), Phillips (Eindhoven, NL).
[4] G. Yu, J. Gao, J. C. Hummelen, F. Wudl, and A. J. Heeger, Science **270**, 1789 (1995).
[5] N. S. Sariciftci, L. Smilowitz, A. J. Heeger, and F. Wudl, Science **258**, 1474 (1992).
[6] N. S. Sariciftci, D. Braun, C. Zhang, V. I. Srdanov, A. J. Heeger, G. Stucky, and F. Wudl, Appl. Phys. Lett. **62**, 585 (1993).
[7] J. J. M. Halls, C. A. Walsh, N. C. Greenham, E. A. Marseglia, R. H. Friend, S. C. Monatti, and A. B. Holmes, Nature (London) **376**, 498 (1995).
[8] M. Granström, K. Petritsch, A. C. Aries, A. Lux, M. R. Andersson, and R. H. Friend, Nature (London) **395**, 257 (1998).
[9] M. R. Andersson, M. Berggren, O. Inganäs, G. Gustafsson, J. C. Gustafsson-Carlberg, D. Selse, T. Hjertberg, and O. Wennerström, Macromolecules **28**, 7525 (1995).
[10] J. Roncali, Chem. Rev. **97**, 173 (1997).
[11] L. Salem, *The Molecular Orbital Theory of Conjugated Systems* (Benjamin, New York, 1966).
[12] J. M. André, J. Delhalle, and J. L. Brédas, *Quantum Chemistry Aided Design of Organic Polymers* (World Scientific, Singapore, 1991).
[13] J. L. Brédas, Synth. Met. **17**, 115 (1987).
[14] F. Wudl, M. Kobayashi, and A. J. Heeger, J. Org. Chem. **49**, 3382 (1984).
[15] For a general overview see: M. Pomerantz, in *Handbook of Conducting Polymers*, 2nd ed., edited by T. A. Skotheim, R. L. Elsenbaumer, and J. R. Reynolds (Marcel Dekker, New York, 1998), p. 278.
[16] S. A. Jenekhe, Nature (London) **322**, 345 (1986).
[17] W.-C. Chen and S. A. Jenekhe, Macromolecules **28**, 454 (1995).
[18] W.-C. Chen and S. A. Jenekhe, Macromolecules **28**, 465 (1995).
[19] M. Kertesz and Y. S. Lee, J. Phys. Chem. **91**, 2690 (1987).
[20] J. Kürti, P. R. Surján, and M. Kertesz, J. Am. Chem. Soc. **113**, 9865 (1991).
[21] R. Kiebooms and F. Wudl, Synth. Met. (in press).
[22] Su-Moon Park, in *Handbook of Organic Conductive Molecules and Polymers*, edited by H. S. Nalwa (Wiley, Chichester, 1997), Vol. 3, p. 429, and references therein.
[23] H. Neugebauer and Z. Ping, Mikrochim. Acta. [Suppl.] **14**, 125 (1997).
[24] H. Neugebauer, Macromol. Symp. **94**, 61 (1995).
[25] H. Neugebauer and N. S. Sariciftci, in *Lower Dimensional Systems and Molecular Electronics*, Nato ASI series, Series B: Physics, edited by R. M. Metzger, P. Day, and G. C. Papavassiliou (Plenum Press, New York, 1991), Vol. 248, p. 401.
[26] TINKER–Software Tools for Molecular Design, Version 3.6 February 1998, Copyright 1990-1998 Jay William Ponder, http://dasher.wustl.edu/tinker
[27] N. L. Allinger, Y. H. Yuh, and J.-H. Lii, J. Am. Chem. Soc. **111**, 8551 (1989).
[28] C. Odin and M. Nechtschein, in *Electronic Properties of Conjugated Polymers III*, Springer Series in Solid-State Sciences, edited by H. Kuzmany, M. Mehring, and S. Roth (Springer, Berlin, Heidelberg, 1989), Vol. 91, p. 172.
[29] G. Tourillon and F. Garnier, J. Electroanal. Chem. Interfacial Electrochem. **161**, 51 (1984).
[30] D. Orata and D. A. Butry, J. Am. Chem. Soc. **109**, 3574 (1987).
[31] G. Zerbi, M. Gussoni, and C. Castiglioni, in *Conjugated Polymers*, edited by J. L. Brédas and R. Silbey (Kluwer, Dordrecht, 1991), p. 435.
[32] B. Horovitz, Solid State Commun. **41**, 729 (1982).
[33] E. Ehrenfreund, Z. Vardeny, O. Brafman, and B. Horovitz, Phys. Rev. B **36**, 1535 (1987).
[34] E. Ehrenfreund and Z. V. Vardeny, Proc. SPIE **3145**, 324 (1997).
[35] A. Girlando, A. Painelli, and Z. G. Soos, J. Chem. Phys. **98**, 7459 (1993).
[36] J. Geisselbrecht, J. Kürti, and H. Kuzmany, Synth. Met. **55–57**, 4266 (1993).
[37] M. Gussoni, C. Castiglioni, and G. Zerbi, in *Spectroscopy of Advanced Materials*, edited by R. J. H. Clark and R. E. Hester (Wiley, New York, 1991),
[38] M. Del Zoppo, C. Castiglioni, P. Zuliani, and G. Zerbi, in *Handbook of Conducting Polymers*, 2nd ed., edited by T. A. Skotheim, R. L. Elsenbaumer, and J. R. Reynolds (Marcel Dekker, New York, 1998), p. 765.
[39] Z. Vardeny, E. Ehrenfreund, O. Brafman, A. J. Heeger, and F. Wudl, Synth. Met. **18**, 183 (1987).
[40] H. Neugebauer, A. Neckel, and N. Brinda-Konopik, in *Electronic Properties of Polymers and Related Compounds*, Springer Series in Solid-State Sciences, edited by H. Kuzmany, M. Mehring, and S. Roth (Springer, Berlin Heidelberg, 1985), Vol. 63, p. 227.
[41] Y. Furukawa, M. Akimoto, and I. Harada, Synth. Met. **18**, 151 (1988).
[42] G. Louarn, J.-Y. Mevellec, J. P. Buisson, and S. Lefrant, Synth. Met. **55–57**, 587 (1993).
[43] G. Zerbi, M. C. Magnoni, I. Hoogmartens, R. Kiebooms, R. Carleer, D. Vanderzande, and J. Gelan, Adv. Mater. **7**, 1027 (1995).
[44] N. S. Sariciftci, M. Mehring, K. U. Gaudl, P. Bäuerle, H. Neugebauer, and A. Neckel, J. Chem. Phys. **96**, 7164 (1992).
[45] H. Eckhardt, L. W. Shacklette, K. Y. Jen, and R. L. Elsenbaumer, J. Chem. Phys. **91**, 1303 (1989).